

Convex Hull Prediction Methods for Bitrate Ladder Construction: Design, Evaluation, and Comparison

Ahmed Telili, Wassim Hamidouche, *Member, IEEE*, Hadi Amirpour, *Member, IEEE*, Sid Ahmed Fezza, Luce Morin, *Member, IEEE* and Christian Timmerer, *Senior Member, IEEE*

Abstract—HTTP adaptive streaming (HAS) has emerged as a prevalent approach for over-the-top (OTT) video streaming services due to its ability to deliver a seamless user experience. A fundamental component of HAS is the bitrate ladder, which comprises a set of encoding parameters (e.g., bitrate-resolution pairs) used to encode the source video into multiple representations. This adaptive bitrate ladder enables the client's video player to dynamically adjust the quality of the video stream in real-time based on fluctuations in network conditions, ensuring uninterrupted playback by selecting the most suitable representation for the available bandwidth. The most straightforward approach involves using a fixed bitrate ladder for all videos, consisting of pre-determined bitrate-resolution pairs known as *one-size-fits-all*. Conversely, the most reliable technique relies on intensively encoding all resolutions over a wide range of bitrates to build the *convex hull*, thereby optimizing the bitrate ladder by selecting the representations from the convex hull for each specific video. Several techniques have been proposed to predict content-based ladders without performing a costly, exhaustive search encoding. This paper provides a comprehensive review of various convex hull prediction methods, including both conventional and learning-based approaches. Furthermore, we conduct a benchmark study of several handcrafted- and deep learning (DL)-based approaches for predicting content-optimized convex hulls across multiple codec settings. The considered methods are evaluated on our proposed large-scale dataset, which includes 300 UHD video shots encoded with software and hardware encoders using three state-of-the-art video standards, including AVC/H.264, HEVC/H.265, and VVC/H.266, at various bitrate points. Our analysis provides valuable insights and establishes baseline performance for future research in this field. The source code of the proposed benchmark and the dataset will be made publicly available upon acceptance of the paper.

Index Terms—Bitrate ladder, video compression, AVC, HEVC, VVC, rate-quality curves, adaptive video streaming, software/hardware encoding.

I. INTRODUCTION

IN recent years, video streaming services, including video on demand (VOD) and live streaming, have become major contributors to internet traffic. A Sandvine report [1] reveals

that video streaming constituted 65.93% of total internet traffic in the first half of 2022. Consequently, video service providers have invested significant resources in optimizing video encoding to enhance the quality of experience (QoE) and ensure seamless streaming performance for all users.

HTTP adaptive streaming (HAS) stands as the state-of-the-art video streaming technology, designed to guarantee the highest possible visual quality delivery at the target bitrate. In HAS, the video content is first split into short chunks, called segments, typically ranging from 2 to 10 seconds. These segments are pre-encoded at various resolutions and quality levels to accommodate a wide range of network conditions, device displays, and computing capabilities. The video segments stored on the server side are transmitted over HTTP to client devices based on their adaptive bitrate (ABR) algorithm [2] requests, which consider their specific bandwidth, display resolution, and computing resource requirements. To facilitate the bitrate selection process for each segment, a bitrate ladder is commonly utilized. The bitrate ladder consists of a set of encoding parameters, often referred to as bitrate-resolution pairs, which indicate the encoding configuration for each video segment. These pairs are organized hierarchically, with higher bitrates associated with higher video quality and resolutions. The primary objective of the bitrate ladder is to provide multiple representations of the video, enabling client devices to dynamically select the highest possible quality while minimizing buffering.

One of the classical approaches to constructing a bitrate ladder is to use a static or *one-size-fits-all* ladder, where a fixed set of bitrate-resolution pairs is used for all video content regardless of their characteristics. While easy to implement, this approach often fails to capture the specific characteristics and complexities of individual videos, potentially leading to suboptimal streaming experiences with either wasted bandwidth or degraded quality due to improper bitrate allocation. As a result, more adaptive and content-aware solutions have been proposed. For example, the per-title encoding solution introduced by Netflix [3] is a content-aware approach that constructs a rate-distortion (RD) curve for each individual title (e.g., movie, TV show). This is achieved by encoding each title at various bitrates and resolutions, with the resulting quality assessed using an objective full-reference video quality metric. Fig. 1 illustrates RD curves for a single video title, where distortion is measured using the video multi-method assessment fusion (VMAF) metric [4]. Subsequently, the convex hull approach was refined with per-shot encoding [5], where each video is segmented into shots with similar frame characteristics that

A. Telili and L. Morin are with Univ. Rennes, INSA Rennes, CNRS, IETR-UMR 6164, Rennes, France (e-mail: {ahmed.telili, luce.morin}@insa-rennes.fr).

A. Telili and W. Hamidouche are with Technology Innovation Institute, P.O.Box: 9639, Masdar City Abu Dhabi, UAE (e-mail: {ahmed.telili, was-sim.hamidouche}@tii.ae).

H. Amirpour and C. Timmerer are with Christian Doppler Laboratory ATHENA, Alpen-Adria-Universitat, Klagenfurt, Austria (e-mail: {hadi.amirpour, christian.timmerer}@aau.at).

SA. Fezza is with the National Higher School of Telecommunications and ICT, Oran, Algeria (e-mail: sfezza@ensttic.dz).

This work has been supported by Région Bretagne under the DEEPTec project.

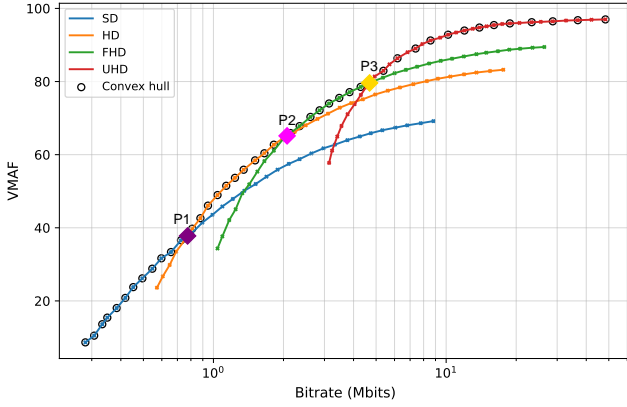


Fig. 1: Example of rate-distortion curves and their convex hull for the sequence of *India-scene-18* from the proposed dataset. P1, P2, and P3 denote the intersection points between SD-HD, HD-FHD, and FHD-UHD resolutions, respectively.

respond similarly to varying encoding parameters. This allows for the creation of customized bitrate ladders for each shot, further optimizing the adaptive convex hull approach. However, generating convex hulls for adaptive streaming, whether per video shot or title, remains computationally expensive due to the vast parameter space encompassing resolution, quality level, codec type, and more. This complexity translates into a time-consuming and resource-intensive process, rendering it costly for VOD streaming and impractical for live streaming scenarios.

To address these challenges, numerous machine learning (ML)-based convex hull prediction techniques have been proposed by both academic and industry experts in recent years [6]–[21]. These techniques aim to predict per-scene or per-shot convex hulls, eliminating the need for exhaustive encoding. In this context, we have conducted a benchmark study that compares various handcrafted- and deep learning (DL)-based methods, providing an in-depth analysis of their complexity and prediction performance. In addition, our benchmark incorporates a multi-codec approach to enhance the evaluation, allowing for a more comprehensive assessment of methods under different encoding scenarios. This comparison and analysis will contribute to a better understanding of the strengths and weaknesses of handcrafted- and DL-based techniques, ultimately guiding the development and comparison of more efficient and adaptable video streaming solutions. The principal contributions of this paper are listed as follows:

- A systematic classification and extensive review of current bitrate ladder construction methods for adaptive video streaming, including a detailed analysis of conventional and learning-based techniques.
- A large dataset with 300 Ultra-HD video sequences, encoded through hardware and software video encoders using three standards: AVC/H.264 [22], HEVC/H.265 [23], and VVC/H.266 [24] in four resolutions and multiple quantization parameter (QP) values.
- Exploring several handcrafted and DL-based features for both VOD and live streaming scenarios with various ML models for convex hull prediction.

- A comprehensive benchmark study to assess the performance of ML-based methods, along with an in-depth analysis of prediction performance and complexity overhead on CPU and GPU platforms.

The remainder of this paper is organized as follows. Section II gives a comprehensive review of bitrate ladder prediction methods. Furthermore, the proposed dataset is presented and characterized in Section II. Section IV presents the development of benchmarking evaluation, while Section V provides and analyses the experimental results. Finally, Section VI concludes this paper.

II. BITRATE LADDER CONSTRUCTION METHODS

This section presents a systematic classification and comprehensive review of existing methods for constructing bitrate ladders in adaptive video streaming. We categorize these methods into two primary classes: (i) static methods, which disregard content characteristics, and (ii) dynamic methods, which involve adaptive selection of bitrate ladders based on content characteristics, network conditions, and other relevant factors. To circumvent computationally intensive brute-force approaches for finding optimal content-aware bitrate ladders, recent dynamic methods typically employ ML techniques to predict the optimized convex hull based on extracted content features. These ML-based approaches are further classified into two types: (a) methods utilizing handcrafted feature extraction and (b) methods employing deep feature extraction relying on deep neural networks.

A. Static methods

The static (*i.e.*, content-independent) bitrate ladder, also known as the *one-size-fits-all* bitrate ladder, is the conventional approach that offers predefined recommendations for encoding parameters, such as bitrate and resolution, for a given video content. Apple proposed one commonly adopted static bitrate ladder in Tech Note TN2224 [25]. Similarly, other video streaming platforms, such as YouTube [26] and Twitch [27], have also provided their recommendations on encoding settings for their streamers. Although these *one-size-fits-all* bitrate ladders are simple to implement and straightforward to use, they have limitations in providing optimal encoding parameters for different types of videos. For complex videos, such as those with high-motion scenes, these static ladders may allocate insufficient bitrate, resulting in significant blocking and other visual artifacts. On the other hand, for less complex video content, such as cartoons, these ladders might over-allocate bitrate, leading to storage and bandwidth wastage. For instance, in Fig. 2, we illustrate the RD curves of 50 video sequences at 1080p resolution, encoded using the x265 software video encoder across a range of qQP values. The figure demonstrates the substantial variability in compression efficiency across different video sequences. Some sequences achieve high Y-peak signal-to-noise ratio (YPSNR) of 45 dB or more at bitrates as low as 1 Mbps, while others require bitrates exceeding 20 Mbps to reach a satisfactory YPSNR of 38 dB. This inherent diversity in video content underscores the limitations of static bitrate ladder schemes, which cannot

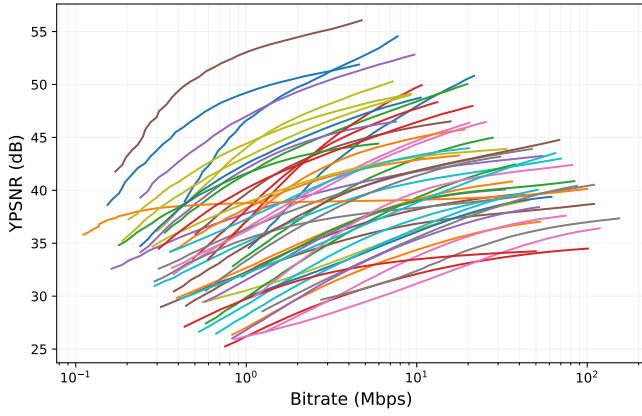


Fig. 2: RD curves for 50 randomly sampled footage at 1080p resolution.

optimally cater to the unique characteristics of individual titles. Consequently, more sophisticated dynamic techniques have been developed to address this challenge.

B. Dynamic methods

In dynamic methods, all parameters of the bitrate ladder, including the number of representations and their corresponding bitrate, resolution, and other encoding parameters, are determined dynamically based on both content characteristics and prevailing network conditions. Netflix pioneered the per-title approach [3], encoding videos at various quality levels and resolutions to construct the convex hull of RD curves using the VMAF metric. This customized bitrate ladder, tailored to each video's unique content, improves the QoE [28] compared to static approaches. As the Netflix service expanded, an optimized per-chunk cloud-based encoding method was introduced [29] for enhanced scalability and reliability. This method identifies suitable bitrate-resolution pairs for each video chunk by evaluating their visual complexity through a constant rate factor (CRF)-based multi-pass encoding process. However, both methods are suboptimal as titles and chunks can contain scenes with varying visual complexity. To address this limitation, Netflix further refined their approach [5] by dividing videos into shots, which are groups of frames with similar encoding behavior. Individual processing of each shot, using the original exhaustive encoding approach, enables the creation of per-shot bitrate ladders. Similarly, Chen *et al.* [30] extracted RD characteristics through multiple encodes of each video chunk at various resolutions and bitrates. Unlike Netflix, this approach considers not only content characteristics but also user bandwidth and viewport size distributions when selecting bitrate-resolution pairs.

Reznik *et al.* [31] introduced an analytical approach that incorporates both content behavior and network statistics to construct the bitrate ladder, formulating it as a nonlinear optimization problem. They utilized the structural similarity index measure (SSIM) [32] as the quality metric and employed probabilistic models to set bitrate constraints. This approach was later extended to accommodate multiple codec types, including AVC/H.264 and HEVC/H.265 [33].

Tashtarian *et al.* [34] developed LALISA, an online lightweight framework for optimizing bitrate ladders in HTTP-based live video streaming. LALISA dynamically determines the optimal bitrate ladder to minimize encoding and delivery costs while maintaining satisfactory QoE during live sessions. Additionally, Amirpour *et al.* [35] proposed the per-title encoding using spatio-temporal resolutions (PSTR) method, incorporating temporal resolution (specifically, framerate) as an additional dimension in bitrate ladder construction. This technique involves encoding each video chunk at multiple resolutions and framerates to identify the optimal settings for each bitrate. While introducing temporal resolution into per-title encoding increases complexity, considering both spatial and temporal resolutions can yield substantial bitrate savings. Further advancing this work, Amirpour *et al.* [36] presented DeepStream, a scalable content-aware per-title encoding system supporting both CPU-only and GPU-equipped users. DeepStream comprises two layers: a base layer that constructs a bitrate ladder using existing per-title encoding methods and an enhancement layer that improves the quality through content-aware deep video super-resolution. This enhancement leverages lightweight context-adaptive binary arithmetic coding (CABAC) for efficient deep neural network (DNN) compression, ensuring backward compatibility for CPU-only users while providing enhanced perceived video quality for those with GPU capabilities. Toni *et al.* [37] proposed a representation set optimization problem for multiview adaptive streaming systems.

C. Learning-based methods

Learning-based methods constitute a class of dynamic techniques that leverage machine learning to identify patterns within input video data, enabling the construction of content-dependent bitrate ladders, specifically convex hulls, without the computational burden of brute-force encoding across all representations. These methods can be broadly categorized into two distinct types based on their feature extraction approach: those employing handcrafted features and those utilizing deep learning for feature extraction.

1) *Handcrafted features*: In learning-based methods, the first class focuses on approaches that leverage handcrafted features. These features are meticulously designed and manually derived from the video content to model. For instance, Bhat *et al.* [7] introduced an innovative approach to swiftly predict adaptive spatial resolutions without requiring multiple encodings. Their algorithm incorporates an extensive array of features, covering rate control-based factors (QP, frame rate, targeted bitrate), spatial features (histogram of pixel values, variance of coding tree unit), temporal features (motion vectors, scene change scores), and encoder pre-analysis-based features (estimated QP of all frames in the initial group of pictures (GOP), estimated intra probability). From the set of features, 43 input features are derived and fed into a machine learning classifier, multilayer perceptron (MLP) or random forest (RF), for resolution prediction.

In [8], the authors introduced a perceptual quality-driven method for generating adaptive encoding ladders. This method

employs the just noticeable difference (JND) scale, representing the smallest perceptible change in visual quality for human viewers. Video sequences are pre-encoded at various resolutions and three QPs per resolution, and features like bitrates, peak signal-to-noise ratio (PSNR), SSIM, and VMAF are extracted. Support vector regression (SVR) is then used to estimate JND scores based on these features, enabling optimization of the encoding ladder to minimize the number of perceptually similar bitrate-resolution pairs.

Menon *et al.* [13] adopted a similar approach in their perceptually-aware online per-title encoding (PPTE) scheme for live streaming. They predict optimal bitrate-resolution pairs for each video segment based on JND, using low-complexity discrete cosine transform (DCT)-energy-based features to assess spatial and temporal complexity. This enables the prediction of bitrates where JNDs occur. Notably, unlike [8], this approach does not rely on pre-encoding, thus accelerating the bitrate ladder construction process.

Katsenou *et al.* [9] introduced a content-agnostic approach using Gaussian processes regression (GPR) to predict cross-over QPs for different spatial resolutions in high-efficiency video coding (HEVC) encoding. The authors employed hand-crafted spatio-temporal features, such as gray level co-occurrence matrix (GLCM) and temporal coherence (TC), extracted from uncompressed ultra high definition (UHD) video sequences to predict QPs based on PSNR. In a subsequent work, Katsenou *et al.* [10] expanded their approach to incorporate the VMAF metric as an additional quality criterion. Similarly, Silhavy *et al.* [11] utilized machine learning algorithms, including SVR, MLP, and random forest regression (RFR), to construct a content-aware bitrate ladder using VMAF as the quality metric. Another handcrafted feature-based method was presented in [12], employing two supervised machine learning algorithms, regression, and a classification method—trained on spatio-temporal features (GLCM, TC) extracted from uncompressed video sequences. An ensemble aggregation technique was applied to predict a bitrate ladder for the versatile video coding (VVC) encoder, enhancing the performance of both ML algorithms. Finally, Menon *et al.* [38] introduced an online resolution prediction approach that leverages low-complexity DCT-energy-based spatio-temporal features extracted from video sequences to predict the optimal resolution for a target bitrate based on these features.

2) *Deep features*: In contrast to methods reliant on hand-crafted features, the deep features category encompasses techniques that leverage DNNs for extracting relevant features from video content. For example, *et al.* [14] proposed DeepLadder, a reinforcement learning-based method that considers video content, network traffic capacity, and storage costs to determine suitable encoder settings for each resolution. Notably, DeepLadder utilizes a pre-trained ResNet-50 model as its backbone for spatial feature extraction from intra-frames.

Furthermore, Xing *et al.* [39] introduced a content-adaptive rate control solution employing a temporal segment network (TSN) [40] to extract spatio-temporal features from video content. These features are then processed by a fully connected layer followed by a Softmax function to predict the optimal rate-control target based on content characteristics. This deep

learning model accommodates both average bitrate control and CRF modes, predicting the optimal bitrate in the former and the rate factor in the latter.

Alternatively, a DNN-based method presented in [41] employs a recurrent convolutional network (RCN) to estimate the convex hull of video shots. This method effectively captures long-term spatio-temporal dependencies across video shots by jointly processing spatial and temporal information using convolutional gated recurrent units (Conv-GRUs) [42]. Notably, the prediction task is formulated as a multi-label classification problem rather than a traditional regression problem. Additionally, a transfer learning technique is employed to mitigate the limited availability of uncompressed public video datasets suitable for training deep models.

Given the data-intensive nature of many learning-based solutions, we dedicate the subsequent section to the construction of a large-scale dataset specifically tailored to support our research objectives.

III. DATASET CONSTRUCTION

A diverse and extensive video dataset is crucial for any data-driven approach. Thus, in this section, we present the adaptive video streaming dataset (AVSD), a comprehensive and diversified collection of 300 UHD video shots from publicly available sources. Additionally, we provide the computed convex hulls for these shots, following encoding using three distinct video coding standards: advanced video coding (AVC)/H.264, HEVC/H.265, and VVC/H.266. We firmly believe that the availability of the AVSD dataset will be of immense value and contribute to the advancement of research in adaptive video streaming and related domains.

A. Video collection

Researchers in the field of learned video compression often face a challenge due to the limited availability of publicly accessible, high-quality, uncompressed video content. To mitigate this issue, we have meticulously curated a dataset of 300 videos, including both uncompressed video sequences and high-quality compressed versions. Within this collection, we have assembled 120 uncompressed video sequences from a variety of sources, including Netflix Chimera [43], AWS Elemental [44], MCML [45], Harmonic [46], Ultra Video Group [47], SJTU [48], and the Waterloo IVC 4K Video Quality Database [49]. The remaining 180 sequences were thoughtfully selected from the YouTube-UGC dataset [50], exclusively featuring high-quality content. While many of these sequences initially boasted a resolution of 4096×2160 , they were subsequently cropped to 3840×2160 and converted into a 4:2:0 chroma subsampled format, if not originally formatted as such. To ensure homogeneity, all sequences underwent a scene segmentation process, guaranteeing that each sequence comprises only a single scene. As a final step, all sequences were temporally cropped to 64 frames, resulting in a dataset that offers a comprehensive view of different scenes and scenarios.

B. Dataset characterization

Winkler *et al.* [51] originally proposed three video descriptors: spatial activity, temporal activity, and colorfulness, to

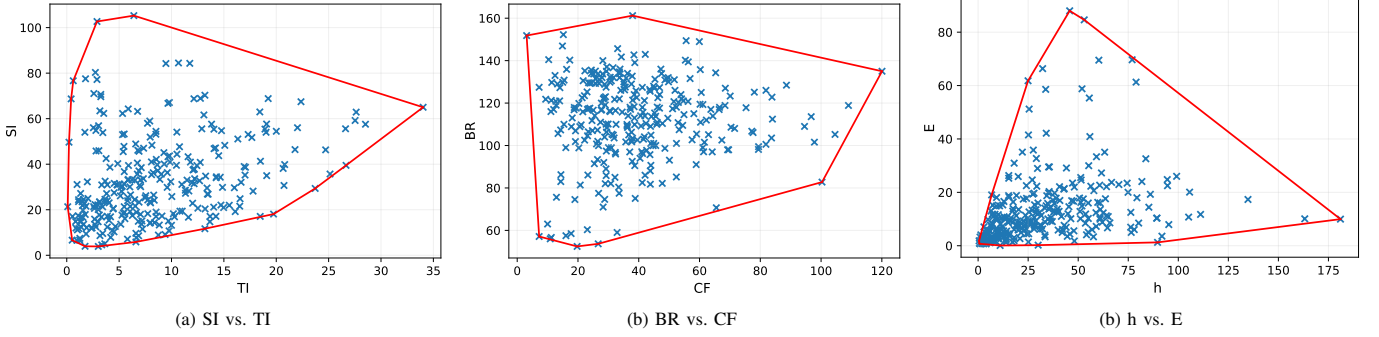


Fig. 3: Source content distribution in paired feature space with corresponding convex hulls. Left column: TI×SI, middle column: CF×BR and right column: h×E.

characterize content diversity within datasets. In our study, we extend this analysis of content diversity by incorporating six low-level features. These features encompass spatial information (SI) [52], temporal information (TI) [52], brightness (BR) [53], colorfulness (CF) [53], and two novel features derived from video complexity analyzer (VCA) [54]: spatial complexity (E) and temporal complexity (h). Each of these features is computed individually for every frame in the dataset. Subsequently, the computed values are averaged to obtain an overall (mean) score. To visualize the feature coverage of our dataset, we present scatter plots with convex hulls for paired features, as depicted in Fig. 3. The video sequences in our dataset span a wide range of the spatio-temporal domain, with SI values ranging from 5 to 105 and TI values from 0 to 35. This diversity extends to the spatio-temporal complexities found within the dataset. The majority of videos exhibit low complexity, characterized by single-shot scenes. However, a smaller fraction contains highly complex shots, adding variety to the dataset. Additionally, the scatter plot of BR versus CF unveils a rich spectrum of content types. BR values span from 60 to 160, indicating diverse lighting conditions and scene settings. Further, CF values range from 0 to 120, signifying a multitude of color palettes and visual styles.

C. Convex hull construction

To determine the RD of video sequences and construct the ground truth bitrate ladder, we downsampled all sequences to full high definition (FHD), high definition (HD), and standard definition (SD) using a Lanczos-3 filter [55]. Subsequently, we encoded the video sequences in four resolutions, which included both the downsampled versions and the original UHD sequences, denoted as $\mathcal{S} \in \{720 \times 480, 1280 \times 720, 1920 \times 1080, 3840 \times 2160\}$. These resolutions represent typical choices in streaming applications [56]. The encoding process was performed using three video coding standards: AVC/H.264, HEVC/H.265, and VVC/H.266. For AVC/H.264 and HEVC/H.265 standards, we employed both software (x264/x265) and hardware-based (NVENC) implementations in random access (RA) configuration, using a range of constant QP values from $\mathcal{Q} \in \{15, 16, \dots, 44, 45\}$ at medium preset. The encoding process for these codecs was conducted using FFmpeg version 5.0 [57]. However, since no public hardware encoder for VVC/H.266 is currently available, we exclusively utilized its

software encoder, Fraunhofer versatile video encoder (VVenC) version 1.6 [58]. Similar to the other codecs, we operated the software encoder in random access configuration with a set of constant QP values from $\mathcal{Q} \in \{16, 18, \dots, 46, 48\}$. This process generated 564 bitstreams per source content, totaling 169,200 encoded video shots. Further, it is essential to mention that the software encoding process was performed on a 16-core, 3.70 GHz Intel Xeon W-2145 CPU with 64 GB RAM, while hardware encoding was performed on an NVIDIA GeForce RTX 2080 Ti GPU. Following this, all the encoded bitstreams underwent a decoding process and were upsampled back to their original resolution (2160p) using the same filter. Subsequently, we proceeded to construct the RD curves. To do this, we measured the objective video quality of the decoded sequences using two full-reference quality metrics: Y-PSNR and VMAF. Finally, we defined the intersection points between the RD curves of the same video across different resolutions to create the convex hull. Specifically, we identified these points as SD-HD, HD-FHD, and FHD-UHD, denoted as P1, P2, and P3, respectively. These points are visually represented in Fig. 1 for a specific video shot encoded with the x264 software encoder. In this study, we address scenarios where direct intersections between RD curves of consecutive resolutions may not occur. We hypothesize that if a resolution \mathcal{S}_{i+1} consistently delivers higher quality than resolution \mathcal{S}_i , the intersection point is defined as the starting bitrate of \mathcal{S}_{i+1} , corresponding to the lowest QP. Conversely, if \mathcal{S}_i remains superior across the bitrate spectrum, we designate the intersection point at a maximum predefined bitrate value.

IV. CONVEX HULL PREDICTION TECHNIQUES

This section describes our benchmark for evaluating learning-based methods for convex hull prediction in adaptive video streaming. The selection of bitrate-resolution pairs from the convex hull is not addressed in this work. We focus on two categories: (i) methods based on handcrafted features and (ii) those based on deep neural networks, aiming to provide valuable insights into their strengths and limitations. These insights aim to guide researchers and practitioners toward more efficient solutions.

A. Methods based on handcrafted features

In this subsection, we examine two sets of handcrafted features for predicting convex hulls. The first set includes

TABLE I: List of VoD-HandC features and their statistics.

Features	Statistics
Grey-Level Co-occurrence Matrix (GLCM)	F1.meanGLCM _{cor} , F2.stdGLCM _{cor} , F3.meanGLCM _{con} , F4.stdGLCM _{con} , F5.meanGLCM _{enr} , F6.stdGLCM _{enr} , F7.meanGLCM _{hom} , F8.stdGLCM _{hom} , F9.meanGLCM _{ent} , F10.stdGLCM _{ent}
Temporal Coherence (TC)	F11.meanTC _{mean} , F12.meanTC _{std} , F13.stdTC _{mean} , F14.stdTC _{std} , F15.meanTC _{skw} , F16.stdTC _{skw} , F17.meanTC _{kur} , F18.stdTC _{kur} , F19.meanTC _{entr} , F20.stdTC _{entr}
Spatial Information (SI)	F21.mean _{SI} , F22.std _{SI}
Temporal Information (TI)	F23.mean _{TI} , F24.std _{TI}
Colorfulness (CF)	F25.mean _{CF} , F26.std _{CF}
Noise estimation	F27.mean _{Noise} , F28.std _{Noise}
Normalized Cross Correlation (NCC)	F29.mean _{NCC} , F30.std _{NCC}

classic low-level features successfully used in compression and video streaming-related research [9], [59], [60]. These classic features, although widely used, are computationally intensive and time-consuming to extract, particularly for UHD videos. Therefore, they are more suitable for VOD streaming applications, hence referred to as VoD-HandC features. On the other hand, the VCA features, referred to as Live-HandC features, aim to provide a more efficient alternative for live-streaming scenarios with real-time and low latency constraints. The results of these methods, including their complexity, will be further explored in Section V.

1) *VoD-HandC features*: The VoD-HandC feature extraction process can be formulated as follows:

$$\mathcal{S}_{F_i} = \Psi_{\text{VoD}}(\mathcal{V}), \quad (1)$$

where \mathcal{S}_{F_i} represents the extracted features set, the Ψ_{VoD} represents VoD-HandC feature extraction function, and \mathcal{V} denotes the input video sequence.

We have selected a set of spatio-temporal features from various low-level features successfully used in our previous related work [60]. Table I provides the full set of these features and their statistics.

GLCM [61] is a spatial feature that analyzes the intensity contrast between adjacent pixels to characterize the texture and patterns in an image. GLCM comprises five fundamental descriptors: contrast, correlation, homogeneity, energy, and entropy.

TC [62] is a temporal feature employed to characterize the predictability of a frame based on its predecessor, assessing the consistency of spectral amplitude between consecutive images to reflect temporal prediction complexity. In practical terms, TC is computed for each pair of successive frames.

SI [52] is a feature employed to gauge the level of spatial detail within an image, encompassing textures, patterns, and structures. SI quantifies the associations among pixel intensity values within an image, offering insights into local variations in the image.

TI [52] is a feature used to evaluate the video's temporal characteristics, such as motion, scene changes, and object dy-

TABLE II: List of Live-HandC features and their statistics.

Features	Statistics
Spatial energy (E)	F1.mean _E , F2.std _E , F3.min _E , F4.max _E , F5.25 th _E , F6.50 th _E , F7.75 th _E , F8.iqr _E , F9.skew _E , F10.kur _E
Temporal energy (h)	F11.mean _h , F12.std _h , F13.min _h , F14.max _h , F15.25 th _h , F16.50 th _h , F17.75 th _h , F18.iqr _h , F19.skew _h , F20.kur _h
Gradient of temporal energy (ε)	F21.mean _ε , F22.std _ε , F23.min _ε , F24.max _ε , F25.25 th _ε , F26.50 th _ε , F27.75 th _ε , F28.iqr _ε , F29.skew _ε , F30.kur _ε
Brightness (BR)	F31.mean _{BR} , F32.std _{BR} , F33.min _{BR} , F34.max _{BR} , F35.25 th _{BR} , F36.50 th _{BR} , F37.75 th _{BR} , F38.iqr _{BR} , F39.skew _{BR} , F40.kur _{BR}

namics. By quantifying the relationships between consecutive frames, TI reveals changes over time.

Colorfulness (CF) [53] is a spatial feature employed to evaluate the richness and diversity of colors within a picture. It quantifies the degree of color variation and saturation, offering insights into the visual appeal and vibrancy of the content.

Noise estimation [63] is a spatial feature employed to evaluate the presence and intensity of noise within an image. It measures the extent of random variations, artifacts, or distortions in pixel values, providing insight into the overall quality and sharpness of the content.

Normalized cross correlation (NCC) [64] is a similarity measure used to assess the temporal similarity between frames based on the correlation of pixel intensity values between two successive frames. To analyze NCC across an entire sequence, the NCC is computed for each pair of consecutive frames.

For each feature, sequence-level statistics are computed to assess the overall characteristics of the video sequence, as indicated in Table I.

2) *Live-HandC features*: While VoD-HandC features have been extensively explored in computer vision and compression-related fields, their extraction is time-consuming, especially for high-resolution videos, limiting real-time applications. This is primarily due to the lack of optimization for online analysis. In response to this issue, Menon *et al.* [54] introduced VCA as an optimized software, leveraging low-complexity features for online video content analysis, ensuring low-latency streaming and improved real-time performance. In this work, we utilize these low-complexity features, referred to as Live-HandC, for which the extraction process can be defined as follows:

$$\mathcal{S}_{F_i} = \Psi_{\text{Live}}(\mathcal{V}), \quad (2)$$

Here, \mathcal{S}_{F_i} represents the set of extracted features, Ψ_{Live} corresponds to the Live-HandC feature extraction module, and \mathcal{V} denotes the input video sequence. The VoD-HandC features are presented below.

Spatial energy (E) is used to quantify the complexity and

TABLE III: Selected features of predicted cross-over bitrates for RD curves based on YPSNR.

Cross-over bitrates	Codec	AVC		HEVC		VVC
	Platform	Software (FFmpeg)	Hardware (NVENC)	Software (FFmpeg)	Hardware (NVENC)	Software (VVenC)
P3	VoD-HandC features	F5, F7, F11, F13, F26, F27, F29	F1, F5, F7, F11, F13, F17, F25-F27, F29	F3, F7, F11-F13, F29, F30, F27	F1, F5, F7, F11-F13, F17, F25-F27, F29	F7, F9, F11, F12, F13, F25, F27, F29
	Live-HandC features	F5, F11, F12, F13, F15, F16, F34, F39	F3, F12, F13, F15, F16, F19, F34	F5, F12, F13, F15, F18, F31, F33, F34, F38	F5, F12, F13, F15, F16, F19, F31, F35, F38	F1, F6, F10, F13, F15, F17, F19, F33, F34, F35-F39
P2	VoD-HandC features	F5, F7, F9-F13, F16, F25-F27, F29	F5, F7, F11, F13, F16, F25, F26, F27, F29	F7, F10, F11, F13, F19, F25, F27, F29	F1, F3, F5, F7-F9, F11-F13, F16, F25-F27, F29, F30	F5, F7, F9-F13, F25, F27, F29
	Live-HandC features	F6, F11-F13, F15, F16, F18, F31, F33, F34, F37-F39	F5, F7, F11-F13, F15, F16, F18, F19, F31, F34, F38, F40	F3, F4, F6, F9, F11, F13, F15, F31, F34, F36, F37, F38, F40	F3, F5, F11-F17, F31, F35, F38, F39	F5, F9, F10, F11, F13, F15, F21, F29, F31, F32, F36, F38, F39
P1	VoD-HandC features	F3, F5-F7, F10-F13, F26, F27, F29	F5, F7, F8, F11, F13, F29	F1-F3, F5, F7, F8, F10-F14, F25, F27, F29	F1, F3, F5-F13, F16, F25-F27, F29, F30	F6-F14, F16, F19, F25, F29, F30
	Live-HandC features	F3, F4, F9-F11, F13, F15, F18, F19, F34, F38	F3-F5, F9, F10, F11, F13, F15, F16, F18, F19, F38, F40	F3, F5, F6, F10, F11, F13-F16, F18, F38	F1, F5, F12-F16, F35, F37, F38, F39	F5, F9, F10, F13, F18, F19, F26, F32, F38, F40

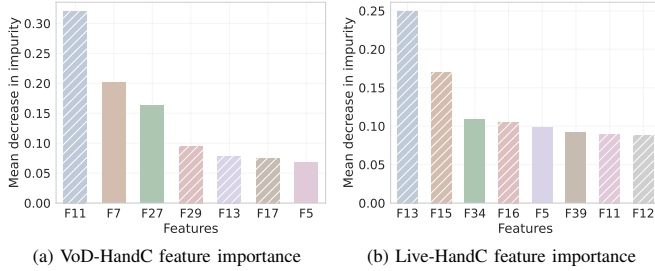


Fig. 4: Feature importance of selected features for P3 cross-point prediction for x264 software encoding in terms of YPSNR. Dashed bars represent temporal features.

variation of textures within an image. It is calculated using a DCT-based energy function that determines the block-wise texture of each frame.

Temporal energy (h) is a temporal feature that measures changes in texture complexity and variation between consecutive frames in a video sequence. The temporal energy is calculated through the sum of absolute differences (SAD) of the texture energy of each frame compared to its previous frame on a block-wise basis.

Gradient of temporal energy (ϵ) is a feature that quantifies the rate of change in texture complexity and variation between consecutive frames in a video sequence. It is calculated as the ratio of the difference between temporal energy (h) values of the $(p-1)^{th}$ and p^{th} frames with the h value of the $(p-1)^{th}$ frame.

Brightness (BR) is a spatial feature that quantifies the overall light intensity of a frame.

Finally, Table II provides the full set of listed features and their statistics. To provide a comprehensive understanding of the entire video, various statistics, such as mean, standard deviation, maximum, minimum, 25th percentile, 50th percentile, 75th percentile, interquartile range (IQR), skewness and kurtosis are computed for each feature.

3) *Feature selection*: In the context of increasing data dimensionality, determining which features to incorporate into machine learning models is crucial. Feature selection addresses this challenge by identifying the most pertinent and informative features within a dataset, thereby (i) enhancing models by reducing dimensionality, (ii) preventing overfitting, and

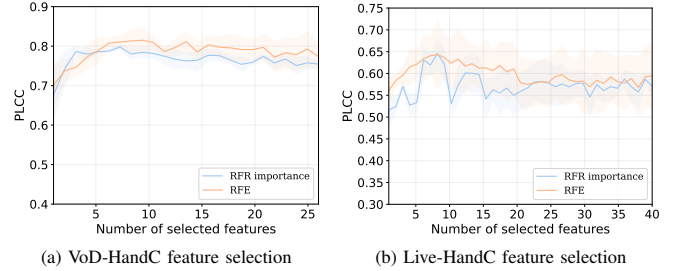


Fig. 5: Feature selection performance (PLCC) for P3 cross-point prediction for x264 software encoding in terms of YPSNR. The shaded error bar represents the standard deviation of PLCC over three iterations.

(iii) lowering computational complexity. In our approach, we employ two types of feature selection algorithms to distill the initial feature set, denoted as \mathcal{SF}_i , into a refined feature set, referred to as \mathcal{SF}_s , for both VoD-HandC and Live-HandC features. This process ensures optimal model efficiency and accuracy. The first type of feature selection employs model-based feature selectors. In this category, we utilize the RFR algorithm, known for its robustness and effectiveness in handling complex datasets. The RFR algorithm fits a regression model, capturing the relationships between features and the target variable. One key advantage of RFR-based feature selectors is their capacity to calculate the permutation importance of each feature, as illustrated in Fig. 4. By ranking the features based on their permutation importance, we can identify and eliminate the least significant ones. The second technique involves applying recursive feature elimination (RFE) to remove the weakest features systematically. The RFE operates by iteratively fitting a machine learning model, ranking features based on their importance, and subsequently eliminating the least important ones. In this study, we utilize ExtraTrees [65] as the target regressor. In the first step, we evaluated both of these feature selection methods on three test-training iterations using stratified sampling. Fig. 5 illustrates the median pearson linear correlation coefficient (PLCC) performance for P3 cross point prediction for x264 software encoding in terms of YPSNR. Following this comparison, we proceeded with the RFE technique due to its superior results. The resulting selected features for predicting cross-over bitrates are presented in Table III for YPSNR RD curves. Finally, these selected features are used to train a regression machine learning model for predicting the

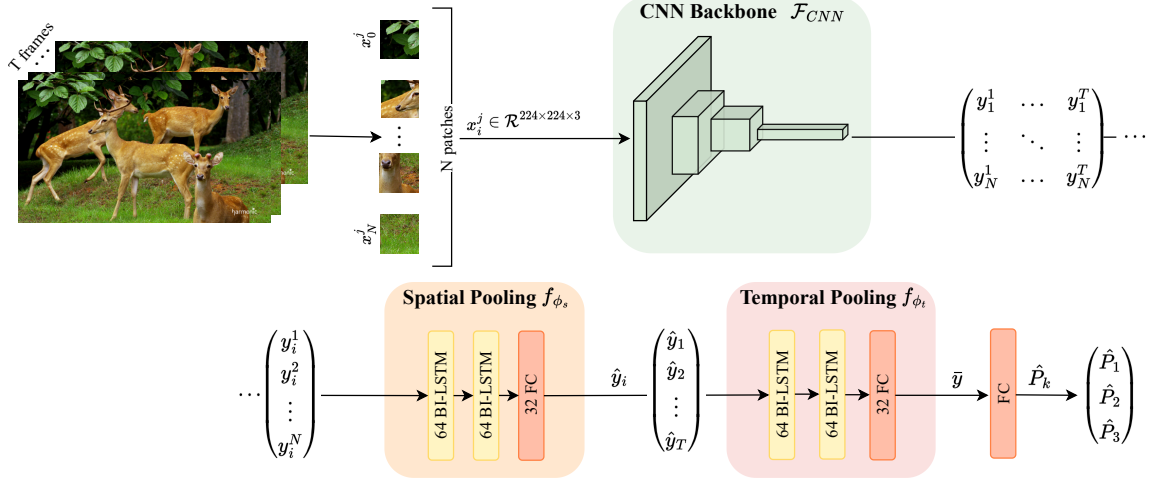


Fig. 6: The overall framework of the proposed DNN methods. The feature extraction module extracts spatial features y_i^j from patches x_i^j . The spatial and temporal pooling modules aggregate features into a final vector \bar{y} . Finally, the regression module uses the final vector \bar{y} to predict the cross-over bitrates \hat{P}_k .

convex hull, as outlined below:

$$\hat{P}_k = \theta_k(\mathcal{S}_{F_s}), \quad (3)$$

where \hat{P}_k denotes the predicted value for P_k on the bitrate ladder $P = (P_1, P_2, P_3)$, θ_k is the parametric function of the regression ML model, while $\mathcal{S}_{F_s} = \{F_1, \dots, F_m\}$ represents the selected feature set.

B. Methods based on deep neural network

Recently, DNNs have gained tremendous attention in computer vision due to their remarkable abilities to process complex visual data and solve a wide range of computer vision problems. In light of these advances, exploring the merit of using deep learning techniques to construct a content-gnostic bitrate ladder in the adaptive video streaming field is well-deserved. Thus, we investigate the application of DNN to achieve this goal in this subsection. As illustrated in Fig. 6, the proposed DNN solution's framework consists of four main modules: feature extraction, spatial pooling, temporal pooling, and convex hull regression module.

1) *Feature extraction*: Deep convolutional neural network (CNN) features offer a more powerful approach than traditional ML-based methods by automatically learning hierarchical representations of local features, enabling the extraction of higher-level abstractions from raw video input. However, the efficacy of CNNs is closely tied to the amount of training data available, and the proposed dataset is still much smaller than the typical computer vision datasets with millions of samples. To enhance feature representation, we used pre-trained models on the extensive ImageNet dataset [66] as backbone models, serving as deep feature descriptors. This leverages the knowledge learned from vast amounts of training data, significantly improving overall the performance of DNN approaches in the context of convex hull prediction.

When using pre-trained models, one challenge is dealing with their fixed input shape requirements. Two potential alternative solutions to address this constraint are resizing the input frame or dividing it into multiple patches. However,

the first method could adversely lead to a loss of fine-grained details and introduce distortions, which may affect the network's ability to extract meaningful features for the accurate prediction of bitrate-resolution pairs. Consequently, we chose the second approach.

Let us consider the input sequence \mathcal{V} as a set of T consecutive frames: $\mathcal{V} = \{x_1, x_2, \dots, x_T\}$. For each frame x_i a sliding window is used to extract N non-overlapping patches x_i^j of size 224×224 , where $j \in \{1, \dots, N\}$ and $i \in \{1, \dots, T\}$. Then, these patches x_i^j are fed into the CNN backbone pre-trained on ImageNet [66] for the extraction of spatial features y_i^j expressed as follows:

$$y_i^j = \mathcal{F}_{CNN}(x_i^j). \quad (4)$$

where \mathcal{F}_{CNN} denotes the CNN backbone.

2) *Spatial pooling*: after extracting features from each patch, they are aggregated into a single vector per frame, encapsulating the frame's spatial information. Traditionally done using spatial pooling, we instead employ a bi-directional long short term memory (Bi-LSTM) network due to the sequential and correlated nature of patches. This approach allows the model to process features in both directions, effectively summarizing local features, reducing computational complexity, and efficiently capturing short-term dependencies between neighboring patches.

The module is composed of two Bi-LSTM layers followed by a fully connected (FC) layer with 256 nodes. We have found that using this architecture leads to the best results in our experiments. The feature vector $(y_i^1, y_i^2, \dots, y_i^N)^T$ of a frame i is fed into the spatial pooling module, expressed as:

$$\hat{y}_i = f_{\phi_s}(y_i^1, y_i^2, \dots, y_i^N), \quad \forall i \in \{1, \dots, T\}, \quad (5)$$

where f_{ϕ_s} is the parametric function of the spatial pooling module with the pooling parameters ϕ_s .

3) *Temporal pooling*: parallel to the spatial aggregation process, temporal aggregation of frame features into a single vector per sequence is also a critical step. This temporal modeling module captures the dynamic changes and patterns

TABLE IV: Performance comparison in YPSNR / VMAF of the considered models on the proposed dataset with AVC encoder. The top result for each encoder type is highlighted in boldface.

Encoder type		AVC software encoding					
Model \ Metric		R2 ↑	SROCC ↑	PLCC ↑	Accuracy ↑	BD-BR vs EEL ↓	BD-BR vs SL ↓
Deep features	VoD-HandC						
	ExtraTrees	0.7265 / 0.5559	0.7466 / 0.7252	0.8689 / 0.7741	0.8462 / 0.8056	2.529% / 4.193%	-6.785% / -7.965%
	Random Forests	0.6760 / 0.5360	0.7114 / 0.6984	0.8308 / 0.7751	0.8309 / 0.7932	2.655% / 4.229%	-6.852% / -7.454%
	XGBoost	0.6629 / 0.5385	0.7263 / 0.6418	0.8241 / 0.6241	0.8395 / 0.7984	2.749% / 4.326%	-6.893% / -7.863%
	LightGBM	0.6143 / 0.5192	0.6472 / 0.6318	0.7925 / 0.7341	0.8235 / 0.8086	2.850% / 4.465%	-5.719% / -6.457%
	Live-HandC						
	ExtraTrees	0.3854 / 0.2869	0.6885 / 0.6209	0.6347 / 0.5671	0.7980 / 0.7558	4.040% / 5.226%	-5.307% / -6.029%
	Random Forests	0.3325 / 0.2429	0.6629 / 0.6072	0.5788 / 0.4399	0.7977 / 0.7589	4.200% / 6.057%	-5.229% / -5.253%
	XGBoost	0.3395 / 0.2417	0.6700 / 0.5905	0.5864 / 0.4951	0.8009 / 0.7483	3.718% / 5.935%	-5.401% / -7.123%
	LightGBM	0.2729 / 0.1745	0.5993 / 0.5114	0.5338 / 0.4327	0.7831 / 0.7350	5.313% / 7.394%	-3.865% / -3.788%
Deep features	DensNet169	0.4964 / 0.5294	0.5487 / 0.6013	0.6813 / 0.7507	0.8032 / 0.7913	3.582% / 5.264%	-5.174% / -6.574%
	VGG16	0.5119 / 0.5133	0.5295 / 0.6000	0.7125 / 0.7373	0.7908 / 0.7845	3.368% / 7.966%	-5.165% / -6.637%
	ResNet-50	0.5416 / 0.5421	0.5371 / 0.6438	0.7425 / 0.7437	0.8155 / 0.7988	2.901% / 4.268%	-6.694% / -7.025%
	ConvNeXtBase	0.5381 / 0.5384	0.5544 / 0.5789	0.7323 / 0.7416	0.7982 / 0.7841	3.323% / 5.678%	-5.489% / -6.051%
Encoder type		AVC hardware encoding					
Model \ Metric		R2 ↑	SROCC ↑	PLCC ↑	Accuracy ↑	BD-BR vs EEL ↓	BD-BR vs SL ↓
Deep features	VoD-HandC						
	ExtraTrees	0.6461 / 0.4431	0.5994 / 0.5451	0.8200 / 0.6885	0.8075 / 0.7856	3.017% / 3.478%	-6.439% / -5.594%
	Random Forests	0.5749 / 0.3289	0.5568 / 0.5152	0.7824 / 0.6343	0.7958 / 0.7719	3.502% / 4.251%	-5.979% / -4.938%
	LightGBM	0.5591 / 0.4706	0.5097 / 0.4561	0.7752 / 0.6231	0.7871 / 0.7565	4.343% / 4.663%	-5.642% / -4.856%
	XGBoost	0.5117 / 0.3207	0.5391 / 0.4696	0.7385 / 0.6073	0.7849 / 0.7507	4.452% / 5.675%	-3.982% / -4.041%
	Live-HandC						
	ExtraTrees	0.2943 / 0.2617	0.5092 / 0.4290	0.5787 / 0.5438	0.7622 / 0.7432	4.547% / 4.606%	-5.292% / -4.512%
	Random Forests	0.2733 / 0.3032	0.4975 / 0.4311	0.5451 / 0.5709	0.7540 / 0.7347	5.523% / 4.892%	-4.352% / -3.952%
	LightGBM	0.2560 / 0.2418	0.4647 / 0.3657	0.5124 / 0.5225	0.7589 / 0.7492	5.363% / 5.453%	-4.605% / -4.152%
	XGBoost	0.1997 / 0.1926	0.4075 / 0.3524	0.4784 / 0.4650	0.7543 / 0.7312	5.920% / 6.253%	-3.105% / -3.573%
Deep features	DensNet169	0.3875 / 0.3880	0.5986 / 0.5275	0.6550 / 0.6592	0.7890 / 0.7811	3.497% / 3.997%	-5.512% / -4.248%
	VGG16	0.4477 / 0.3849	0.6023 / 0.5095	0.6871 / 0.6431	0.7921 / 0.7663	3.678% / 3.999%	-5.041% / -3.812%
	ResNet-50	0.5534 / 0.4152	0.6048 / 0.5567	0.7042 / 0.6462	0.7940 / 0.7803	3.249% / 3.807%	-5.754% / -4.502%
	ConvNeXtBase	0.5116 / 0.4033	0.5601 / 0.4737	0.7022 / 0.6349	0.7967 / 0.7716	3.320% / 3.932%	-5.605% / -4.277%

over time, providing a crucial dimension of information for predicting the bitrate ladder. Hence, we employ a temporal modeling module that utilizes a Bi-LSTM network to consolidate the frame-level features, denoted as $(\hat{\mathbf{y}}_1, \hat{\mathbf{y}}_2, \dots, \hat{\mathbf{y}}_T)$, into a comprehensive global feature vector $\bar{\mathbf{y}}$ that encapsulates the entire video sequence. Bi-LSTM networks are adept at considering both forward and backward information, enabling the capture of long-range dependencies among frames. Analogous to the spatial modeling, this module comprises two Bi-LSTM layers, each with 64 cells, and is subsequently followed by a FC layer containing 256 nodes. The temporal modeling module can be expressed as follows:

$$\bar{\mathbf{y}} = f_{\phi_t}(\hat{\mathbf{y}}_1, \hat{\mathbf{y}}_2, \dots, \hat{\mathbf{y}}_T), \quad (6)$$

where f_{ϕ_t} is the parametric function of the temporal modeling module with the training parameters ϕ_t .

4) *Convex hull regression*: following the extraction and aggregation of deep features into a single representative vector $\bar{\mathbf{y}}$, the challenge lies in mapping these features onto the respective point in the final convex hull. To address this, we employed one node in a FC layer as a regression model with a linear activation function to predict a single point on the convex hull. To predict the complete bitrate ladder, $P = (P_1, P_2, P_3)$, we implemented three distinct models, each consisting of a spatial and temporal module as described above, followed by the regression module. We have found that using this architecture, with separate models for each point on the convex hull, leads to the best results in our experiments.

Consequently, the prediction for each point in the convex hull can be formulated as follows:

$$\hat{P}_k = \zeta_k(\bar{\mathbf{y}}), \quad (7)$$

where \hat{P}_k represents the predicted value for P_k on the bitrate ladder $P = (P_1, P_2, P_3)$ and ζ_k denotes the FC layer, where $k \in \{1, 2, 3\}$.

The training process is performed with 200 epochs using Adam optimizer [67] with an initial learning rate of $1e-4$, batch size of 16 and the Mean Squared Error (MSE) as loss function. All backbones are frozen during this process, and the rest of the network is trained.

V. EXPERIMENTAL RESULTS

In this section, we first define the experimental setup, including the baselines, the evaluation methods, and the implementation details. Then, we present the coding performance in terms of coding efficiency and complexity.

A. Experimental setup

1) *Baselines*: due to the lack of publicly available implementations for many of the methods discussed in Section II, we opted to benchmark the performance of our proposed models against two alternative methods. These methods, outlined below, offer a trade-off between computational cost, simplicity, and compression performance:

TABLE V: Performance comparison in YPSNR / VMAF of the considered models on the proposed dataset with HEVC encoder. The top result for each encoder type is highlighted in boldface.

Encoder type		HEVC software encoding					
Model \ Metric		R2 ↑	SROCC ↑	PLCC ↑	Accuracy ↑	BD-BR vs EEL ↓	BD-BR vs SL ↓
Deep features \ VoD-HandC	ExtraTrees	0.6479 / 0.4929	0.6730 / 0.6286	0.8154 / 0.7131	0.8852 / 0.8685	1.776% / 2.545%	-5.997% / -5.583%
	Random Forests	0.6079 / 0.4293	0.6452 / 0.6087	0.7847 / 0.6679	0.8814 / 0.8626	2.365% / 2.670%	-5.886% / -5.721%
	XGBoost	0.5659 / 0.3877	0.6312 / 0.5867	0.7767 / 0.6541	0.8775 / 0.8606	2.909% / 3.331%	-5.524% / -4.943%
	LightGBM	0.5487 / 0.4095	0.6436 / 0.5762	0.7518 / 0.6496	0.8665 / 0.8397	2.023% / 3.841%	-5.293% / -4.785%
Deep features \ Live-HandC	ExtraTrees	0.2700 / 0.3250	0.4941 / 0.5341	0.5411 / 0.5832	0.8354 / 0.8396	3.448% / 4.037%	-4.805% / -5.179%
	Random Forests	0.2627 / 0.2301	0.5083 / 0.5363	0.5303 / 0.5060	0.8329 / 0.8303	3.870% / 4.310%	-4.784% / -4.803%
	XGBoost	0.2507 / 0.1920	0.5181 / 0.4978	0.5317 / 0.4471	0.8303 / 0.8299	3.866% / 4.041%	-4.828% / -4.585%
	LightGBM	0.2438 / 0.1687	0.5172 / 0.4279	0.5088 / 0.4169	0.8315 / 0.8149	3.840% / 4.188%	-4.889% / -4.531%
Deep features	DensNet169	0.3306 / 0.3139	0.3778 / 0.5374	0.5703 / 0.5250	0.8793 / 0.8395	3.300% / 3.181%	-4.915% / -4.823%
	VGG16	0.2787 / 0.2511	0.3832 / 0.5531	0.5767 / 0.5083	0.8637 / 0.8227	3.378% / 3.329%	-4.845% / -4.751%
	ResNet-50	0.5652 / 0.3204	0.5057 / 0.5802	0.6349 / 0.5400	0.8805 / 0.8539	2.755% / 2.999%	-5.387% / -5.012%
	ConvNeXtBase	0.3188 / 0.2321	0.4788 / 0.4650	0.5884 / 0.5005	0.8756 / 0.8252	3.600% / 3.434%	-4.892% / -4.712%
Encoder type		HEVC hardware encoding					
Model \ Metric		R2 ↑	SROCC ↑	PLCC ↑	Accuracy ↑	BD-BR vs EEL ↓	BD-BR vs SL ↓
Deep features \ VoD-HandC	ExtraTrees	0.4728 / 0.3822	0.5927 / 0.4424	0.7027 / 0.6452	0.8373 / 0.7815	2.644% / 4.850%	-5.319% / -5.068%
	Random Forests	0.4113 / 0.3481	0.5475 / 0.3934	0.6527 / 0.6057	0.8278 / 0.7800	3.292% / 4.724%	-4.896% / -4.932%
	XGBoost	0.4139 / 0.2794	0.5219 / 0.3452	0.6536 / 0.5462	0.8228 / 0.7669	3.880% / 5.370%	-4.916% / -4.472%
	LightGBM	0.3039 / 0.1876	0.5304 / 0.3347	0.6428 / 0.4816	0.8029 / 0.7371	4.501% / 5.915%	-4.922% / -3.728%
Deep features \ Live-HandC	ExtraTrees	0.3188 / 0.2321	0.4788 / 0.4650	0.5884 / 0.5005	0.7894 / 0.7715	4.610% / 5.100%	-4.209% / -3.533%
	Random Forests	0.2854 / 0.1866	0.4879 / 0.3989	0.5612 / 0.4020	0.7841 / 0.7613	5.205% / 5.921%	-3.951% / -3.258%
	XGBoost	0.2490 / 0.1391	0.4843 / 0.3629	0.5293 / 0.4686	0.7793 / 0.7627	5.049% / 5.930%	-4.094% / -2.807%
	LightGBM	0.3039 / 0.1876	0.5304 / 0.3347	0.6428 / 0.4816	0.8029 / 0.7371	4.501% / 5.915%	-4.922% / -3.728%
Deep features	DensNet169	0.3750 / 0.4408	0.5710 / 0.5477	0.6109 / 0.7133	0.8272 / 0.8143	3.059% / 4.333%	-4.967% / -5.018%
	VGG16	0.3422 / 0.3559	0.5584 / 0.4899	0.6159 / 0.6239	0.7649 / 0.7529	3.750% / 5.335%	-4.807% / -3.931%
	ResNet-50	0.3466 / 0.4229	0.5965 / 0.5251	0.6354 / 0.7025	0.8278 / 0.8003	2.811% / 4.150%	-5.139% / -5.533%
	ConvNeXtBase	0.2440 / 0.3490	0.5013 / 0.5127	0.5284 / 0.6253	0.7420 / 0.7544	3.916% / 5.417%	-4.745% / -3.590%

Exhaustive encoding ladder (EEL): this approach, based on exhaustive encoding detailed in Subsection III-C, provides a reference point for our performance measurements by generating a fully specialized convex hull for each content. The EEL approach also serves as the ground truth during the training stage.

Static ladder (SL): this method creates a fixed bitrate resolution pair by averaging the ground truth bitrate ladders obtained from the training dataset (using the EEL approach).

2) *Considered models:* In our benchmark, we consider two sets of handcrafted features and four deep features extracted from popular deep CNN models: VGG16 [68], DenseNet169 [69], ResNet-50 [70], and ConvNeXtBase [71]. The two sets of handcrafted features, VoD-HandC and Live-HandC, are trained with four machine-learning regression algorithms, including ExtraTrees Regressor [65], Random Forest [72], XGBoost [73], and LightGBM [74], resulting in eight handcrafted-based models. The deep features are processed with the spatial and temporal pooling models described in Section IV-B, resulting in four DL-based methods.

3) *Evaluation metrics:* for a comprehensive evaluation, we split the AVSD dataset into two non-overlapping subsets, 80% for training and the remaining 20% for testing. To minimize sampling bias and ensure the representation of all types of content, we employed stratified sampling, repeating this process three times to mitigate the impact of sampling errors. To assess the performance of the considered models, we used three correlation metrics, including R-squared (R2),

spearman rank order correlation coefficient (SROCC), and PLCC, to measure the correlation between the predicted cross-over bitrates and the reference cross-over bitrates generated by the EEL approach. We also use the accuracy to evaluate the performance of each approach in predicting the optimal resolution over all tested bitrates. Finally, we compute the bjøntegaard delta bitrate (BD-BR) score between the predicted and the reference bitrate ladders, giving the rate gain or loss in percentage of each method compared to the anchor. This is done by encoding video sequences at various bitrates, with their resolutions defined by both ladders, and then using the resulting bitrate and quality values to determine the BD-BR.

B. Coding performance

Tables IV, V, and VI give the median performance of the considered models over three stratified iterations on the AVSD dataset, using the AVC, HEVC, and VVC encoders, respectively for both YPSNR and VMAF objective quality metrics.

Table IV shows the performance of these models using AVC software and hardware encoders. The VoD-HandC features-based models consistently achieve high scores across multiple metrics in both encoding scenarios. For instance, the ExtraTrees Regressor model achieves an average accuracy of 88%/86% in predicting cross-over bitrates, resulting in a gain of 5.99%/5.58% over the static approach at the cost of a slight BD-BR loss of 1.77%/2.54% compared to the EEL method using software encoding, in terms of YPSNR/VMAF. The

TABLE VI: Performance comparison in YPSNR / VMAF of the considered models on the proposed dataset with VVC encoder. The top result for each encoder type is highlighted in boldface.

Encoder type		VVC software encoding					
Model \ Metric		R2 \uparrow	SROCC \uparrow	PLCC \uparrow	Accuracy \uparrow	BD-BR vs EEL \downarrow	BD-BR vs SL \downarrow
VoD-HandC	ExtraTrees	0.5093 / 0.3379	0.6696 / 0.5896	0.7217 / 0.6249	0.9267 / 0.8030	2.685% / 3.701%	-5.184% / -4.900%
	Random Forests	0.5057 / 0.2622	0.5661 / 0.5251	0.7351 / 0.5654	0.9211 / 0.7908	3.389% / 5.051%	-4.777% / -3.487%
	XGBoost	0.4813 / 0.2096	0.5746 / 0.5471	0.7065 / 0.5431	0.9232 / 0.7968	3.448% / 4.546%	-4.692% / -4.811%
	LightGBM	0.3722 / 0.2354	0.5439 / 0.5031	0.6147 / 0.5218	0.9060 / 0.7989	4.009% / 4.827%	-4.596% / -3.888%
Live-HandC	ExtraTrees	0.2613 / 0.1144	0.5447 / 0.4741	0.5611 / 0.2921	0.8936 / 0.7792	3.714% / 4.751%	-3.890% / -3.413%
	Random Forests	0.2021 / 0.0511	0.5222 / 0.4541	0.4700 / 0.2500	0.8858 / 0.7662	3.863% / 5.682%	-3.764% / -3.256%
	XGBoost	0.2210 / 0.0540	0.5351 / 0.4503	0.4777 / 0.2705	0.8894 / 0.7708	3.886% / 5.395%	-3.750% / -3.831%
	LightGBM	0.1208 / 0.0470	0.3641 / 0.3612	0.3655 / 0.2606	0.8777 / 0.7594	5.218% / 5.533%	-2.903% / -2.984%
Deep features	DensNet169	0.3998 / 0.3280	0.4281 / 0.4924	0.6286 / 0.5966	0.9018 / 0.7665	3.215% / 4.871%	-3.957% / -3.563%
	VGG16	0.3861 / 0.3066	0.4069 / 0.5027	0.6288 / 0.5821	0.8990 / 0.7676	3.606% / 4.775%	-4.012% / -3.464%
	ResNet-50	0.4220 / 0.3174	0.4472 / 0.5712	0.6407 / 0.5903	0.9144 / 0.7815	3.099% / 4.658%	-4.067% / -4.190%
	ConvNeXtBase	0.3860 / 0.2702	0.4373 / 0.5510	0.6264 / 0.5293	0.9047 / 0.7702	3.126% / 4.801%	-3.892% / -3.392%

Live-HandC features-based models (VCA features), although not as strong as the VoD-HandC features, still outperform the SL approach, resulting in an average BD-BR gain of 4.95%/5.54% with software encoding and 4.33%/4.04% with hardware encoding, in terms of YPSNR/VMAF. On the other hand, DNN-based models show relatively competitive performance compared to the VoD-HandC features-based models, particularly ResNet-50, which achieved the best results among CNN baselines in both software and hardware encoding scenarios. Fig. 7 illustrates the histogram of BD-BR per tested sequence compared to EEL and SL methods. The figure shows that the bitrate gain is content dependent, ranging from -30% gain to a slight loss for a few sequences (outliers) compared to the SL method.

Table V presents the performance comparison using the HEVC encoders. The VoD-HandC feature-based (VoD-HandC) models exhibit strong performance in HEVC software encoding, notably with the ExtraTrees Regressor model achieving the highest scores in terms of YPSNR and VMAF. It outperforms the static approach with an overall gain of 5.99%/5.58% while incurring only a slight loss of 1.77%/2.54% compared to the EEL method in terms of BD-BR. Additionally, the Live-HandC feature-based (Live-HandC) models perform consistently better than the static approach SL, particularly the ExtraTrees Regressor, with an average BD-BR gain of 4.80%/5.17% using software encoding and 4.20%/3.53% using hardware encoding. In comparison, the DNN-based models, particularly ResNet-50, show competitive performance, achieving the best results among the CNN baselines in both software and hardware encoding scenarios.

Table VI compares the performance of the models considered using the VVC software encoder. Among the models considered, the ExtraTrees model, fitted with VoD-HandC features, stands out, as it achieves the highest performance in terms of YPSNR and VMAF. It outperforms the static approach with an overall gain of 5.18%/4.90% in YPSNR/VMAF while only incurring a loss of 2.86%/3.70% compared to the EEL method in terms of BD-BR. Furthermore, the Live-HandC feature-based models consistently perform better than the static approach SL, with an average BD-BR gain of 3.89%/3.41% for the best model. In terms of DNN-based mod-

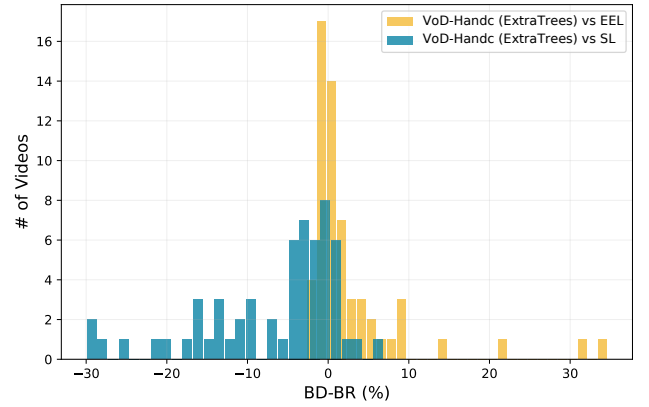


Fig. 7: Histogram of BD-BR for VoD-HandC ExtraTrees model compared to EEL and SL approaches for AVC software encoding in terms of YPSNR.

els, as expected, ResNet-50 outperforms all CNN baselines with accuracy in predicting cross-over bitrates of 91%/78% in term of YPSNR.

In summary, VoD-HandC feature-based models consistently performed well across different encoding scenarios. The Live-HandC feature-based models also showed superiority over the static approach. Further, DNN-based models, particularly ResNet-50, demonstrated competitive performance compared to VoD-HandC feature-based models, which can be further optimized with a more extensive training dataset.

C. Runtime Comparison

Computational complexity is a critical consideration for constructing bitrate ladders in both VOD and live adaptive streaming applications. We conducted runtime comparisons of the evaluated models on a desktop computer equipped with an Intel® Xeon(R) W-2133 CPU @3.60GHz \times 12, 64GB RAM, and a GeForce RTX 2080 Ti GPU, running Ubuntu 20.04 LTS. Table VII presents the average inference time in seconds, measured over ten random UHD video sequences from the AVSD dataset, for both CPU and GPU implementations.

The results indicate that Live-HandC feature-based models achieve remarkably fast feature extraction times, requiring less

TABLE VII: Average inference runtime (Seconds) comparison evaluated on 10 UHD videos.

Model		Features extraction		Prediction	
		CPU	GPU	CPU	GPU
VoD-HandC	ExtraTrees	144.754	✗	0.0011	✗
	Randomforest	144.754	✗	0.0006	✗
	XGboost	144.754	✗	0.0005	✗
	LightGBM	144.754	✗	0.0003	✗
Live-HandC	ExtraTrees	1.086	✗	0.0013	✗
	Randomforest	1.086	✗	0.0008	✗
	XGboost	1.086	✗	0.0006	✗
	LightGBM	1.086	✗	0.0005	✗
Deep features	DensNet169	304.877	69.041	0.1720	0.0888
	VGG16	473.982	67.363	0.1403	0.0625
	ResNet50	273.211	63.636	0.2157	0.1013
	ConvexNetBase	11729.184	146.996	0.1541	0.0744

than 1.1 seconds. Furthermore, the prediction time for these methods is even shorter, ranging from 2 to 13 milliseconds on CPU. This demonstrates the suitability of Live-HandC features (VCA features) for real-time live streaming scenarios where low latency is paramount. Conversely, VoD-HandC feature-based models exhibit a longer feature extraction time of approximately 145 seconds, making them better suited for VOD streaming. It's worth noting that software optimization of the feature extraction process could potentially reduce time complexity.

Deep learning models also exhibit extended feature extraction times. For example, ResNet50 requires approximately 273 seconds on CPU and 63 seconds on GPU. However, DNN models can be further optimized to reduce inference time through techniques such as pruning and knowledge distillation [75].

VI. CONCLUSION

In this paper, we have undertaken a comprehensive review of existing methods for constructing bitrate ladders in adaptive video streaming. These methods are categorized into two main approaches: static and dynamic. Additionally, we have curated an extensive collection of video shots and have developed the largest publicly available dataset of corresponding convex hulls, referred to as AVSD. These convex hulls were generated by encoding the shots using both hardware and software video encoders, encompassing three standards: AVC/H.264, HEVC/H.265, and VVC/H.266, across four resolutions and various QP values. Furthermore, we have presented an empirical benchmark study focusing on learning-based methods for convex hull prediction. The experimental results demonstrate that the ExtraTrees Regressor, fitted with VoD-HandC hand-crafted features, outperforms other learning-based methods when predicting cross-over bitrates. However, it is worth noting that these features can be computationally expensive and time-consuming, particularly when dealing with UHD videos, making them more suitable for VOD streaming scenarios. Moreover, our complexity analysis reveals that models based on Live-HandC features are the most suitable for live streaming applications. These features strike a balance between inference runtime and prediction performance, making

them an efficient choice for such scenarios. Additionally, the promising performances of baseline CNN models suggest the significant potential of DNN approaches in addressing adaptive streaming challenges. We believe this comprehensive benchmarking study will significantly contribute to and facilitate future research endeavors in the domain of bitrate ladder prediction for adaptive video streaming.

REFERENCES

- [1] Sandvine, "Global Internet Phenomena Report 2022," <https://www.sandvine.com/phenomena>, accessed on 2023-01-30.
- [2] A. Bentalb, B. Taani, A. C. Begen, C. Timmerer, and R. Zimmermann, "A Survey on Bitrate Adaptation Schemes for Streaming Media Over HTTP," *IEEE Commun. Surveys Tuts.*, vol. 21, no. 1, pp. 562–585, 2019.
- [3] (2015) Per-Title Encode Optimization. [Online]. Available: <https://netflixtechblog.com/per-title-encode-optimization-7e99442b62a2>
- [4] "VMAF: The Journey Continues. by Zhi Li, Christos Bampis | by Netflix Technology Blog | Netflix TechBlog." [Online]. Available: <https://netflixtechblog.com/vmaf-the-journey-continues-44b51ee9ed12>
- [5] I. Katsavounidis. (2018) Dynamic Optimizer — A Perceptual Video Encoding Optimization Framework. [Online]. Available: <https://netflixtechblog.com>
- [6] K. Goswami *et al.*, "Adaptive Multi-Resolution Encoding for ABR Streaming," in *2018 25th IEEE International Conference on Image Processing (ICIP)*. IEEE, 2018, pp. 1008–1012.
- [7] M. Bhat, J.-M. Thiesse, and P. Le Callet, "A Case Study of Machine Learning Classifiers for Real-Time Adaptive Resolution Prediction in Video Coding," in *IEEE International Conference on Multimedia and Expo (ICME)*, 2020.
- [8] M. Takeuchi *et al.*, "Perceptual Quality Driven Adaptive Video Coding Using JND Estimation," in *Picture Coding Symposium (PCS)*, 2018.
- [9] A. V. Katsenou, J. Sole, and D. R. Bull, "Content-agnostic Bitrate Ladder Prediction for Adaptive Video Streaming," in *Picture Coding Symposium (PCS)*, 2019.
- [10] A. V. Katsenou, F. Zhang, K. Swanson, M. Afonso, J. Sole, and D. R. Bull, "VMAF-Based Bitrate Ladder Estimation for Adaptive Streaming," in *Picture Coding Symposium (PCS)*, 2021.
- [11] D. Silhavy *et al.*, "Machine Learning for Per-Title Encoding," *SMPTE Motion Imaging Journal*, vol. 131, no. 3, pp. 42–50, 2022.
- [12] F. Nasiri, W. Hamidouche, L. Morin, N. Dholand, and J.-Y. Aubié, "Ensemble Learning for Efficient VVC Bitrate Ladder Prediction," in *European Workshop on Visual Information Processing (EUVIP)*, 2022.
- [13] V. V. Menon, H. Amirpour, M. Ghanbari, and C. Timmerer, "Perceptually-Aware Per-Title Encoding for Adaptive Video Streaming," in *IEEE International Conference on Multimedia and Expo (ICME)*, 2022.
- [14] T. Huang, R.-X. Zhang, and L. Sun, "Deep Reinforced Bitrate Ladders for Adaptive Video Streaming," in *ACM Workshop on Network and Operating Systems Support for Digital Audio and Video*, 2021.
- [15] (2020) Per-title encoding. [Online]. Available: <https://bitmovin.com/per-title-encoding>
- [16] G. Gao, H. Zhang, H. Hu, Y. Wen, J. Cai, C. Luo, and W. Zeng, "Optimizing quality of experience for adaptive bitrate streaming via viewer interest inference," *IEEE Trans. on Multimedia*, vol. 20, no. 12, pp. 3399–3413, 2018.
- [17] W. Li, J. Huang, W. Lyu, B. Guo, W. Jiang, and J. Wang, "Rav: Learning-based adaptive streaming to coordinate the audio and video bitrate selections," *IEEE Trans. on Multimedia*, vol. 25, pp. 5662–5675, 2023.
- [18] S. Meng, J. Sun, Y. Duan, and Z. Guo, "Adaptive video streaming with optimized bitstream extraction and pid-based quality control," *IEEE Trans. on Multimedia*, vol. 18, no. 6, pp. 1124–1137, 2016.
- [19] A. Bokani, M. Hassan, S. Kanhere, and X. Zhu, "Optimizing http-based adaptive streaming in vehicular environment using markov decision process," *IEEE Trans. on Multimedia*, vol. 17, no. 12, pp. 2297–2309, 2015.
- [20] T. Feng, H. Sun, Q. Qi, J. Wang, and J. Liao, "Vabis: Video adaptation bitrate system for time-critical live streaming," *IEEE Trans. on Multimedia*, vol. 22, no. 11, pp. 2963–2976, 2020.
- [21] A. Telili, W. Hamidouche, S. A. Fezza, and L. Morin, "Efficient per-shot transformer-based bitrate ladder prediction for adaptive video streaming," in *2023 IEEE International Conference on Image Processing (ICIP)*, 2023, pp. 1835–1839.

- [22] T. Wiegand, G. J. Sullivan, G. Bjontegaard, and A. Luthra, "Overview of the H. 264/AVC Video Coding Standard," *IEEE Trans. Circuits Sys. Video Technol.*, vol. 13, no. 7, pp. 560–576, 2003.
- [23] G. J. Sullivan, J.-R. Ohm, W.-J. Han, and T. Wiegand, "Overview of the High Efficiency Video Coding (HEVC) Standard," *IEEE Trans. Circuits Sys. Video Technol.*, vol. 22, no. 12, pp. 1649–1668, 2012.
- [24] B. Bross, Y.-K. Wang, Y. Ye, S. Liu, J. Chen, G. J. Sullivan, and J.-R. Ohm, "Overview of the Versatile Video Coding (VVC) Standard and its Applications," *IEEE Trans. Circuits Sys. Video Technol.*, vol. 31, no. 10, pp. 3736–3764, 2021.
- [25] (2021) Best Practices for Creating and Deploying HTTP Live Streaming Media for the iPhone and iPad. [Online]. Available: https://developer.apple.com/documentation/http_live_streaming/http_live_streaming_hls_authoring_specification_for_apple_devices
- [26] YouTube: Choose Live Encoder Settings, Bitrates, and Resolutions. [Online]. Available: <https://support.google.com/youtube/answer/2853702>
- [27] Twitch. [Online]. Available: <https://stream.twitch.tv/>
- [28] H. Zhang, L. Dong, G. Gao, H. Hu, Y. Wen, and K. Guan, "DeepQoE: A Multimodal Learning Framework for Video Quality of Experience (QoE) Prediction," *IEEE Transactions on Multimedia*, vol. 22, no. 12, pp. 3210–3223, Dec. 2020. [Online]. Available: <https://ieeexplore.ieee.org/document/8999528/>
- [29] J. De Cock, Z. Li, M. Manohara, and A. Aaron, "Complexity-Based Consistent-Quality Encoding in the Cloud," in *IEEE International Conference on Image Processing (ICIP)*, 2016, pp. 1484–1488.
- [30] C. Chen, Y.-C. Lin, S. Bunting, and A. Kokaram, "Optimized Transcoding for Large Scale Adaptive Streaming Using Playback Statistics," in *IEEE International Conference on Image Processing (ICIP)*, 2018.
- [31] Y. A. Reznik, K. O. Lillevold, A. Jagannath, J. Greer, and J. Corley, "Optimal Design of Encoding Profiles for ABR Streaming," in *Proceedings of the 23rd Packet Video Workshop*, 2018, pp. 43–47.
- [32] Z. Wang, A. C. Bovik, H. R. Sheikh, and E. P. Simoncelli, "Image quality assessment: from error visibility to structural similarity," *IEEE Trans. Image Process.*, vol. 13, no. 4, pp. 600–612, 2004.
- [33] Y. A. Reznik, X. Li, K. O. Lillevold, A. Jagannath, and J. Greer, "Optimal Multi-Codec Adaptive Bitrate Streaming," in *IEEE International Conference on Multimedia & Expo Workshops (ICMEW)*, 2019.
- [34] F. Tashtarian, A. Bentalah, H. Amirpour, B. Taraghi, C. Timmerer, H. Hellwagner, and R. Zimmermann, "LALISA: Adaptive Bitrate Ladder Optimization in HTTP-based Adaptive Live Streaming," in *IEEE/IFIP Network Operations and Management Symposium (NOMS)*, 2023.
- [35] H. Amirpour, C. Timmerer, and M. Ghanbari, "PSTR: Per-Title Encoding Using Spatio-Temporal Resolutions," in *IEEE International Conference on Multimedia and Expo (ICME)*, 2021.
- [36] H. Amirpour, M. Ghanbari, and C. Timmerer, "DeepStream: Video Streaming Enhancements using Compressed Deep Neural Networks," *IEEE Trans. Circuits Sys. Video Technol.*, 2022.
- [37] L. Toni and P. Frossard, "Optimal Representations for Adaptive Streaming in Interactive Multiview Video Systems," *IEEE Transactions on Multimedia*, vol. 19, no. 12, pp. 2775–2787, Dec. 2017. [Online]. Available: <http://ieeexplore.ieee.org/document/7944625/>
- [38] V. V. Menon, H. Amirpour, M. Ghanbari, and C. Timmerer, "OPTE: Online Per-Title Encoding for Live Video Streaming," in *ICASSP 2022*, May 2022, pp. 1865–1869, iSSN: 2379-190X.
- [39] H. Xing, Z. Zhou, J. Wang, H. Shen, D. He, and F. Li, "Predicting Rate Control Target Through A Learning Based Content Adaptive Model," in *IEEE Picture Coding Symposium (PCS)*, 2019.
- [40] L. Wang, Y. Xiong, Z. Wang, Y. Qiao, D. Lin, X. Tang, and L. Van Gool, "Temporal Segment Networks: Towards Good Practices for Deep Action Recognition," in *European conference on computer vision*. Springer, 2016, pp. 20–36.
- [41] S. Paul, A. Norkin, and A. C. Bovik, "Efficient Per-Shot Convex Hull Prediction By Recurrent Learning," *arXiv preprint arXiv:2206.04877*, 2022.
- [42] N. Ballas, L. Yao, C. Pal, and A. Courville, "Delving Deeper Into Convolutional Networks for Learning Video Representations," *arXiv preprint arXiv:1511.06432*, 2015.
- [43] I. Katsavounidis, "Chimera Video Sequence Details and Scenes," https://www.cdv1.org/documents/NETFLIX_Chimera_4096x2160_download_instructions.pdf, 2015.
- [44] A. Elemental, https://www.youtube.com/playlist?list=PLWlpNY17SOG_C5176Tf46n6ImKssMn2kT/, [Online; accessed 2018-07-02].
- [45] M. Cheon and J.-S. Lee, "Subjective and Objective Quality Assessment of Compressed 4K UHD Videos for Immersive Experience," *IEEE Trans. Circuits Sys. Video Technol.*, vol. 28, no. 7, pp. 1467–1480, 2017.
- [46] Harmonic Inc 4K Demo Footage, <https://www.harmonicinc.com/4k-demo-footage-download/>, [Online; accessed 2017-05-01].
- [47] T. U. Ultra Video Group, <http://ultravideo.cs.tut.fi/>, [Online; accessed 2017-01-23].
- [48] L. Song, X. Tang, W. Zhang, X. Yang, and P. Xia, "The SJTU 4K Video Sequence Dataset," in *IEEE International Workshop on Quality of Multimedia Experience (QoMEX)*, 2013, pp. 34–35.
- [49] Z. Li, Z. Duanmu, W. Liu, and Z. Wang, "AVC, HEVC, VP9, AVS2 OR AV1?—A Comparative Study of State-of-the-Art Video Encoders on 4K Videos," in *International Conference on Image Analysis and Recognition*. Springer, 2019, pp. 162–173.
- [50] Y. Wang, S. Inguva, and B. Adsumilli, "YouTube UGC Dataset for Video Compression Research," in *IEEE International Workshop on Multimedia Signal Processing (MMSP)*.
- [51] S. Winkler, "Analysis of Public Image and Video Databases for Quality Assessment," *IEEE Journal of Selected Topics in Signal Processing*, vol. 6, no. 6, pp. 616–625, 2012.
- [52] International Telecommunication Union, "ITU-T Recommendation P.910: Subjective Video Quality Assessment Methods for Multimedia Applications," ITU-T, Recommendation, 2008. [Online]. Available: <https://www.itu.int/rec/T-REC-P.910>
- [53] M. D. Fairchild, *Color Appearance Models*. John Wiley & Sons, 2013.
- [54] V. V. Menon, C. Feldmann, H. Amirpour, M. Ghanbari, and C. Timmerer, "VCA: Video Complexity Analyzer," in *Proceedings of the 13th ACM Multimedia Systems Conference*, 2022, pp. 259–264.
- [55] C. E. Duchon, "Lanczos Filtering in One and Two Dimensions," *Journal of Applied Meteorology and Climatology*, vol. 18, no. 8, pp. 1016–1022, 1979.
- [56] Dacast, <https://www.dacast.com/blog/adaptive-bitrate-streaming/>, [Online; accessed 2023-03-02].
- [57] FFmpeg. [Online]. Available: <https://www.ffmpeg.org/>
- [58] A. Wieckowski *et al.*, "VVenC: An Open and Optimized VVC Encoder Implementation," in *IEEE International Conference on Multimedia & Expo Workshops (ICMEW)*, 2021.
- [59] M. Afonso, F. Zhang, and D. R. Bull, "Spatial Resolution Adaptation Framework for Video Compression," in *Applications of Digital Image Processing XLI*, vol. 10752. SPIE, 2018, pp. 209–218.
- [60] A. Telili, W. Hamidouche, S. A. Fezza, and L. Morin, "Benchmarking Learning-Based Bitrate Ladder Prediction Methods for Adaptive Video Streaming," in *Picture Coding Symposium (PCS)*, 2022, pp. 325–329.
- [61] R. M. Haralick, K. Shanmugam, and I. H. Dinstein, "Textural Features for Image Classification," *IEEE Trans. Syst., Man, Cybern.*, no. 6, pp. 610–621, 1973.
- [62] A. V. Katsenou, M. Afonso, D. Agrafiotis, and D. R. Bull, "Predicting Video Rate-Distortion Curves Using Textural Features," in *Picture Coding Symposium (PCS)*, 2016.
- [63] C. Liu, W. T. Freeman, R. Szeliski, and S. B. Kang, "Noise Estimation from A Single Image," in *IEEE Computer Society Conference on Computer Vision and Pattern Recognition (CVPR'06)*, vol. 1, 2006, pp. 901–908.
- [64] J. P. Lewis, "Fast Template Matching," in *Vision interface*, vol. 95, no. 120123. Quebec City, QC, Canada, 1995, pp. 15–19.
- [65] P. Geurts, D. Ernst, and L. Wehenkel, "Extremely Randomized Trees," *Machine learning*, vol. 63, pp. 3–42, 2006.
- [66] J. Deng, W. Dong, R. Socher, L.-J. Li, K. Li, and L. Fei-Fei, "Imagenet: A Large-Scale Hierarchical Image Database," in *IEEE conference on computer vision and pattern recognition*, 2009, pp. 248–255.
- [67] D. P. Kingma and J. Ba, "Adam: A Method for Stochastic Optimization," in *3rd International Conference on Learning Representations, ICLR 2015, San Diego, CA, USA, May 7-9, 2015, Conference Track Proceedings*, Y. Bengio and Y. LeCun, Eds., 2015.
- [68] X. Zhang, J. Zou, K. He, and J. Sun, "Accelerating Very Deep Convolutional Networks for Classification and Detection," *IEEE Trans. Pattern. Anal. Mach. Intell.*, vol. 38, no. 10, pp. 1943–1955, 2015.
- [69] G. Huang, Z. Liu, L. Van Der Maaten, and K. Q. Weinberger, "Densely Connected Convolutional Networks," in *IEEE conference on computer vision and pattern recognition*, 2017, pp. 4700–4708.
- [70] K. He, X. Zhang, S. Ren, and J. Sun, "Deep Residual Learning for Image Recognition," in *IEEE conference on computer vision and pattern recognition*, 2016, pp. 770–778.
- [71] Z. Liu, H. Mao, C.-Y. Wu, C. Feichtenhofer, T. Darrell, and S. Xie, "A Convnet for the 2020s," in *IEEE/CVF Conference on Computer Vision and Pattern Recognition*, 2022, pp. 11 976–11 986.
- [72] T. K. Ho, "Random Decision Forests," in *IEEE international conference on document analysis and recognition*, vol. 1, 1995, pp. 278–282.
- [73] T. Chen *et al.*, "XGBoost: Extreme Gradient Boosting," *R package version 0.4-2*, vol. 1, no. 4, pp. 1–4, 2015.

- [74] G. Ke, Q. Meng, T. Finley, T. Wang, W. Chen, W. Ma, Q. Ye, and T.-Y. Liu, “Lightgbm: A Highly Efficient Gradient Boosting Decision Tree,” *Advances in neural information processing systems*, vol. 30, 2017.
- [75] C. Morris, D. Danier, F. Zhang, N. Anantrasirichai, and D. R. Bull, “Stmfnet mini: Knowledge distillation-driven frame interpolation,” in *2023 IEEE International Conference on Image Processing (ICIP)*, 2023, pp. 1045–1049.